



Brilliant Violet[™] Antibody Conjugates
Superior Performance for the Violet Laser



The Early Marginal Zone B Cell-Initiated T-Independent Type 2 Response Resists the Proteasome Inhibitor Bortezomib

This information is current as of October 4, 2011

Veronika R. Lang, Dirk Mielenz, Kirsten Neubert, Christina Böhm, Georg Schett, Hans-Martin Jäck, Reinhard E. Voll and Silke Meister

J Immunol 2010;185;5637-5647; Prepublished online 4 October 2010;

doi:10.4049/jimmunol.1001040

<http://www.jimmunol.org/content/185/9/5637>

-
- References** This article **cites 36 articles**, 13 of which can be accessed free at: <http://www.jimmunol.org/content/185/9/5637.full.html#ref-list-1>
- Subscriptions** Information about subscribing to *The Journal of Immunology* is online at <http://www.jimmunol.org/subscriptions>
- Permissions** Submit copyright permission requests at <http://www.aai.org/ji/copyright.html>
- Email Alerts** Receive free email-alerts when new articles cite this article. Sign up at <http://www.jimmunol.org/etoc/subscriptions.shtml/>

The Journal of Immunology is published twice each month by The American Association of Immunologists, Inc., 9650 Rockville Pike, Bethesda, MD 20814-3994. Copyright ©2010 by The American Association of Immunologists, Inc. All rights reserved. Print ISSN: 0022-1767 Online ISSN: 1550-6606.



The Early Marginal Zone B Cell-Initiated T-Independent Type 2 Response Resists the Proteasome Inhibitor Bortezomib

Veronika R. Lang,^{*,†} Dirk Mielenz,^{*,‡} Kirsten Neubert,^{*,†} Christina Böhm,^{*,†,§}
Georg Schett,^{*,§} Hans-Martin Jäck,^{*,‡} Reinhard E. Voll,^{*,†,§,1} and Silke Meister^{*,†,1}

The proteasome inhibitor bortezomib is approved for the treatment of multiple myeloma and mantle cell lymphoma. We recently demonstrated that bortezomib eliminates autoreactive plasma cells in systemic lupus erythematosus mouse models, thereby representing a promising novel treatment for Ab-mediated diseases. In this study, we investigated the effects of bortezomib on the just developing and pre-existing T-dependent Ab response toward dinitrophenyl-keyhole limpet hemocyanin and the T-independent type 2 response toward (4-hydroxy-3-iodo-5-nitrophenyl)acetyl (NIP)-Ficoll in BALB/c mice. Bortezomib treatment strongly reduced T-dependent Ab titers mainly due to depletion of plasma cells. In contrast, the early T-independent type 2 response against i.v. administered NIP-Ficoll, which is predominantly dependent on marginal zone (MZ) B cells, resisted bortezomib. Upon bortezomib treatment, immunoproteasome subunits and the antiapoptotic unfolded protein response including NF- κ B were induced in NIP-Ficoll-stimulated MZ B cells, but not in plasma cells and follicular B cells. In summary, bortezomib treatment decreases Ab titers arising from T-dependent immune responses predominantly by eliminating plasma cells. In contrast, the early T-independent type 2 response protecting the organism against blood-borne pathogens remains largely intact due to a remarkable resistance of MZ B cells against proteasome inhibition. *The Journal of Immunology*, 2010, 185: 5637–5647.

The first clinically approved proteasome inhibitor bortezomib (Velcade) is successfully used for the treatment of relapsed multiple myeloma and mantle cell lymphoma (1). The use of bortezomib in other malignancies is currently investigated in clinical trials (2). Bortezomib inhibits the chymotrypsin-like activity of the 26S proteasome, a proteolytic complex that degrades most cellular proteins, including cell cycle regulators and signaling molecules (3). Importantly, the proteasome is involved in the regulation of NF- κ B activity, because proteasomal degradation of its inhibitors, the I κ B proteins, is required for NF- κ B activation. NF- κ B drives the expression of several antiapoptotic and oncogenic factors (4).

We reported recently for mouse models of systemic lupus erythematosus that bortezomib efficiently depletes short- and long-lived plasma cells, with the latter being resistant to conventional therapies, and it markedly ameliorates the disease course (5). The selective elimination of plasma cells producing huge

amounts of secreted Igs can mainly be explained by the induction of endoplasmic reticulum (ER) stress by accumulation of misfolded translational products upon proteasome blockade (6). ER stress activates the unfolded protein response (UPR) to ensure cell survival by activation of the ER-associated degradation pathway, attenuation of translation, and induction of chaperones and survival factors such as NF- κ B (7). However, if the adaptive mechanisms fail to compensate overwhelming ER stress, the terminal UPR leads to apoptosis (8). Toxic effects on cells that neither synthesize large amounts of proteins nor rapidly proliferate are uncommon (9).

In this study, we compared the influence of bortezomib on early and late phases of T-dependent and T-independent type 2 Ab responses. Unlike the other B cell subsets and plasma cells during T-dependent responses, marginal zone (MZ) B cells, which play an important role in the T-independent first-line defense against blood-borne pathogens such as encapsulated bacteria (10), were completely resistant against bortezomib. Upon Ag encounter, MZ B cells differentiate into large numbers of plasmablasts within hours and produce huge amounts of IgM Abs (11, 12). We expected that the drastic increase of Ab synthesis upon (4-hydroxy-3-iodo-5-nitrophenyl)acetyl (NIP)-Ficoll stimulation should render activated MZ B cells sensitive to bortezomib. However, the numbers of MZ B cells remained unchanged, and IgM levels to the T-independent type 2 Ag even increased upon bortezomib administration. We provide evidence that induction of immunoproteasomes, the absence of terminal UPR activation, and persisting activation of NF- κ B may contribute to the resistance of MZ B cells to bortezomib. Thus, proteasome inhibition might not cause relevant impairment of first-line immune responses against blood-borne pathogens such as encapsulated bacteria.

Materials and Methods

Treatment of mice

Mouse experiments were approved by the Government of Mittelfranken. BALB/c mice (6–8 wk old) were purchased from Janvier (Le Genest-St-

^{*}Department of Internal Medicine 3, [†]Clinical Research Group, [‡]Division of Molecular Immunology, and [§]Institute of Clinical Immunology, Nikolaus-Fiebiger Center, University of Erlangen–Nuremberg, Erlangen, Germany

¹R.E.V. and S.M. contributed equally to this work.

Received for publication March 30, 2010. Accepted for publication August 6, 2010.

This work was supported in part by grants from the Interdisciplinary Center for Clinical Research (IZKF, Project N2, and a stipend to V.L.), the German Research Society (FOR 831 TP 8; VO673/31), and the Collaborative Research Centers (SFB 643; Project B3).

Address correspondence and reprint requests to Dr. Reinhard E. Voll and Dr. Silke Meister, Nikolaus-Fiebiger Center of Molecular Medicine, Department of Internal Medicine 3 and Institute of Clinical Immunology, University of Erlangen–Nuremberg, Glückstrasse 6, 91054 Erlangen, Germany. E-mail addresses: rvoll@molmed.uni-erlangen.de and frey.silke@web.de

Abbreviations used in this paper: BW, body weight; Bz, bortezomib; Bz 0, bortezomib from day 0; Bz 8, bortezomib from day 8; DNP, dinitrophenyl; ER, endoplasmic reticulum; FB, follicular B cells; KLH, keyhole limpet hemocyanin; MZ, marginal zone; NIP, (4-hydroxy-3-iodo-5-nitrophenyl)acetyl; PC BM, plasma cells from the bone marrow; PC spleen, plasma cells from the spleen; RT, reverse transcriptase; UPR, unfolded protein response.

Copyright © 2010 by The American Association of Immunologists, Inc. 0022-1767/10/\$16.00

Isle, France). To examine the effect of bortezomib on the T-dependent response, mice were immunized i.p. with 100 μ g dinitrophenyl (DNP)-keyhole limpet hemocyanin (KLH) (Calbiochem, La Jolla, CA) diluted in PBS, adding an equal volume of IFA (Sigma-Aldrich, Steinheim, Germany) to a total volume of 500 μ l. After 14 d, mice were boosted with 100 μ g DNP-KLH. To assess the effect of bortezomib on the ongoing immune response, groups of six mice were treated i.v. with 0.75 mg/kg body weight (BW) bortezomib (Velcade; Janssen-Cilag, Neuss, Germany) beginning simultaneously with the first immunization and then twice weekly for 56 d. Controls received PBS. Another group of mice was injected i.v. with PBS for 28 d before starting bortezomib treatment (late treatment). Serum samples were obtained every 14 d. After 56 d mice were sacrificed.

To analyze the T-independent type 2 response, mice were immunized i.v. with 25 μ g NIP-Ficoll (Biosearch Technologies, Novato, CA) diluted in PBS to a total volume of 150 μ l. To assess the effect of bortezomib on the early phase of the response to NIP-Ficoll, mice were treated i.v. with 0.75 mg/kg BW bortezomib on days 0, 3, and 5. After 5 d mice were sacrificed. Alternatively, mice were treated i.v. with bortezomib simultaneously with the immunization twice weekly for 16 d. Controls received PBS. Another group of mice received PBS for 8 d and then was treated i.v. with bortezomib from day 8 twice weekly. Serum samples were taken before and on days 5, 10, and 15 after the immunization. At day 16 mice were sacrificed.

Flow cytometric analyses

Single-cell suspensions from spleens and bone marrows (femora) were obtained as previously described (13). Flow cytometric analyses were performed using fluorochrome-conjugated mAbs to mouse CD4, CD5, CD8, CD11a, CD11b, CD11c, CD21, CD23, CD25, CD69, CD138, c-kit, IgD, IgM, κ -L chain, λ -L chain (all from BD Biosciences, Heidelberg, Germany), F4/80, CD45R (B220) (both from Caltag Laboratories, Hamburg, Germany), and biotin-conjugated CD69 (Jackson ImmunoResearch Laboratories, West Grove, PA). For the staining of germinal center B cells, peanut hemagglutinin (Vector Laboratories, Burlingame, CA) was used. For the analyses of plasma cells and plasmablasts, intracellular κ - and λ -L chains and intracellular IgM, respectively, were stained using the Fix and Perm cell permeabilization kit (Caltag Laboratories) according to the manufacturer's instructions. Cytofluorometric analyses were performed on a FACSCalibur and analyzed using CellQuest software (both from BD Biosciences). Total cell numbers were calculated by multiplication of percentages of respective subpopulations, with the cell counts obtained from total spleens or bone marrow of femora. We based the calculation of the total bone marrow cell numbers on previous investigations showing that both femoral bones contain ~8% of total bone marrow cells of a mouse (5).

ELISPOT assays

To assess cells secreting IgG Abs to DNP-KLH, 96-well multiscreen plates (Millipore, Billerica, MA) were coated with 2 μ g/ml DNP-KLH. Cell suspensions of spleens and bone marrow were prepared and 2×10^5 splenocytes or 2×10^5 bone marrow cells were incubated in dodecaplicates for 2 h at 37°C in a humidified incubator containing 5% CO₂. After incubation, cells were washed away and the plates were incubated with HRP-conjugated goat anti-mouse IgG (Jackson ImmunoResearch Laboratories) for 1 h at 20°C. Bound IgG specific to DNP-KLH was stained by addition of tetramethylbenzidine one-component membrane peroxidase (Kirkegaard & Perry Laboratories, Gaithersburg, MD). The numbers of spots were counted with a video-based automatic ELISPOT reader (AID Diagnostics, Strassberg, Germany). To quantify total IgG-secreting cells, plates were coated with goat anti-mouse IgG (SouthernBiotech, Birmingham, AL). Serial dilutions of splenocytes and bone marrow cells starting with 2×10^5 cells were incubated in the same manner. Total membrane-bound IgG was detected as described above. Controls included cells from a nonimmunized mouse.

ELISA

Sandwich ELISAs were performed in triplicates on 96-well microplates (Thermo Fisher Scientific, Roskilde, Denmark). To quantify concentrations of IgM, IgG, and IgG subclasses, plates were coated with goat anti-mouse antisera (1 μ g/ml; all from SouthernBiotech), and bound Abs were detected with HRP-conjugated goat anti-mouse secondary Abs (SouthernBiotech). The Ig concentrations were calculated using standard curves of purified IgG, IgA, and IgM Abs (SouthernBiotech). For the analysis of DNP-KLH-specific Abs, plates were coated with 2 μ g/ml DNP-KLH. In a first set of experiments, optimal sera dilutions were determined. According to these results, sera were diluted 1:1000 to analyze anti-DNP-KLH IgM and 1:2000 to assess anti-DNP-KLH IgG. To detect anti-NIP-

Abs, plates were coated with 2 μ g/ml NIP-BSA (Biosearch Technologies). Sera were diluted 1:200 to detect anti-NIP-IgM and 1:100 to analyze anti-NIP-IgG. The amounts of DNP-KLH-specific IgM and IgG Abs were quantified with HRP-conjugated goat anti-mouse secondary Abs (SouthernBiotech). *o*-Phenylenediamine dihydrochloride (Sigma-Aldrich, Taufkirchen, Germany) was used as substrate. OD was measured at 495 nm in a SpectraMax 190 ELISA reader (Molecular Devices, Ismaning, Germany).

Isolation of plasma cells and plasmablasts

Mice were immunized with DNP-KLH as described above. After 14 d splenocytes and bone marrow cells were isolated. Plasma cells were stained with Abs to CD138 and Fc γ RIIB (BD Biosciences), plasmablasts were stained with Abs to CD138 and IgM, and cells were sorted with a purity >95% by a MoFlo cell sorter (Dako, Boxborough, MA). Anti-CD25 was used to exclude pre-B cells. To assess transcriptional changes after bortezomib treatment, mice were once injected i.v. with 1 mg/kg BW bortezomib or PBS and sacrificed 4 h later.

Isolation of MZ and follicular B cells

Mice were immunized i.v. with 25 μ g NIP-Ficoll. After 5 d splenocytes were isolated. Cells were stained with Abs to B220 (CD45R), CD21, and CD23. MZ B cells were sorted using a MoFlo cell sorter as B220⁺/CD21^{high}/CD23^{low} population, and follicular B cells were sorted as B220⁺/CD21^{low}/CD23^{high} population, both with a purity >98%. To assess the effect of bortezomib, mice were once injected i.v. with 1 mg/kg BW bortezomib or PBS and sacrificed 4 h later.

RNA and cDNA preparation

The Qiagen Mini RNAeasy kit (Qiagen, Hilden, Germany) was used for the isolation of total RNA. DNA digestion was performed with RNase-free DNase (Qiagen). First-strand cDNA synthesis was performed with the SuperScript III reverse transcriptase (RT) first-strand synthesis system (Invitrogen, Karlsruhe, Germany). cDNA integrity was checked by PCR of β -actin.

Real-time PCR

cDNA was used as template for relative RT-real-time PCR reactions with corresponding primers (all retrieved from the Harvard PrimerBank at <http://pga.mgh.harvard.edu/primerbank/>): Bax forward, 5'-TGAAGACAGGG-GCCTTTTGG-3', Bax reverse, 5'-AATTCGCCGAGACACTCG-3'; Bcl-2 forward, 5'-ATGCCTTTGTGGAACATATATGGC-3'; Bcl-2 reverse, 5'-GGTATGCACCCAGAGATGC-3'; BiP forward, 5'-ACTTGGGGAC-CACCTATTCCT-3'; BiP reverse, 5'-ATCGCCAATCAGACGCTCC-3'; CHOP forward, 5'-CTGGAAGCCTGGTATGAGGAT-3'; CHOP reverse, 5'-CAGGGTCAAGAGTAGTGAAGGT-3'; I κ B α forward, 5'-TGAAG-GACGAGGATACGAGC-3'; I κ B α reverse, 5'-TTCGTGGATGATTGC-CAAGTG-3'; β -actin forward, 5'-GGCTGTATTCCCCTCCATCG-3'; β -actin reverse, 5'-CCAGTTGGTAACAATGCCATGT-3'; LMP2 forward, 5'-CTTGCTGCTTCTGTGCTCG-3'; LMP2 reverse, 5'-GCCACTGCA-GGGAGTACAT-3'; LMP7 forward, 5'-CACTGCCATGATGGTGTCT-3'; LMP7 reverse, 5'-ACTACCCCGTAGGCAAGGT-3'; PSMB5 forward 5'-CCACAGCAGGTGCTTATATTGC-3'; PSMB5 reverse, 5'-GCTCATAG-ATTCCGACTGCC-3'; and absolute quantitative RT-PCR SYBR Green ROX reagent (Thermo Fisher Scientific/Abgene, Hamburg, Germany). Relative real-time PCR was performed in triplicates for each sample in an Applied Biosystems 7300 real-time PCR system (Applied Biosystems, Darmstadt, Germany). cDNA obtained from RNA prepared of a pool of total splenocytes was used as reference to calculate the relative amounts of mRNA.

Measurement of proteasomal activity

Sorted plasma cells, plasmablasts, and MZ and follicular B cells (2×10^4 cells each) were disseminated in pentaplicates. The chymotrypsin-like proteasomal activity was detected using the luminogenic proteasome substrate-based Proteasome-Glo chymotrypsin-like cell-based assays kit (Promega, Madison, WI) according to the manufacturer's instructions. A 96-well SpectraMax 190 plate reader (Molecular Devices, Sunnyvale, CA) was used for measurement.

Immunoblotting

NIP-Ficoll-immunized mice were once injected i.v. with 1 mg/kg BW bortezomib or PBS and sacrificed after 8 h. Sorted 5×10^5 follicular and MZ B cells were washed with PBS and directly lysed in SDS sample buffer containing 2-ME to generate total cell lysates. The following primary Abs were used: mouse monoclonal anti-actin (Sigma-Aldrich, Taufkirchen, Ger-

many), mouse monoclonal anti-GRP78 (BiP) (BD Pharmingen, Heidelberg, Germany), rabbit polyclonal anti-CHOP (Santa Cruz Biotechnology, Santa Cruz, CA), rabbit polyclonal anti-proteasome 20S LMP2, rabbit polyclonal anti-proteasome 20S LMP7 (both from Novus Biologicals, Littleton, CO). As secondary Abs we used HRP-conjugated goat anti-mouse IgG and goat anti-rabbit IgG (Jackson ImmunoResearch Laboratories). Membranes were blocked with 5% nonfat dry milk (Roth, Karlsruhe, Germany), probed with Abs, and developed using the ECL method. HeLa cells treated with 8 μ g/ml tunicamycin for 6 h (Sigma-Aldrich, Taufkirchen, Germany), commonly used to induce UPR, served as control.

Mobilization of MZ B cells into the peripheral blood

MZ B cells of NIP-Ficoll-immunized mice were released into the peripheral blood by i.v. injection of 0.1 mg rat anti-mouse CD49d/VLA-4 Abs (clone PS/2; Biozol, Eching, Germany) and 0.1 mg rat anti-mouse CD11a (integrin α -L chain, LFA-1 α -chain) mAb (clone M17/4; BD Pharmingen). Mice were simultaneously treated i.v. with 1 mg/kg BW bortezomib or PBS, respectively. Controls received the same volume of PBS instead of the anti-integrin Abs and were injected i.v. with bortezomib or PBS in the same manner.

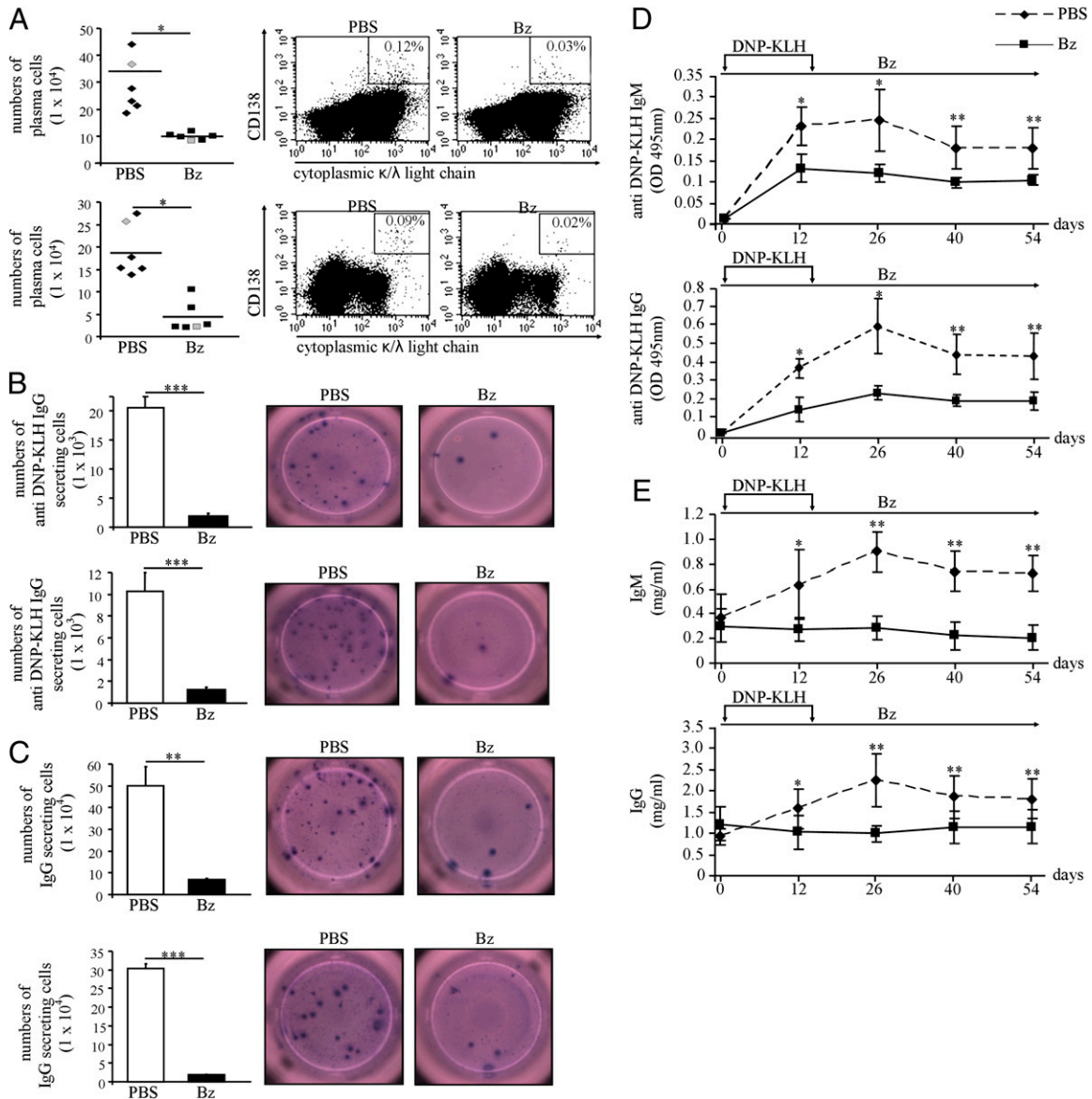


FIGURE 1. Inhibition of the T-dependent response toward DNP-KLH upon bortezomib treatment beginning with immunization. Mice were immunized twice with DNP-KLH at intervals of 14 d and treated with bortezomib every 72 h for 56 d. *A*, Total numbers and representative dot plots of CD138⁺/cytoplasmic κ/λ -L chain⁺/CD25⁻ plasma cells in the spleen (*upper panel*) and the bone marrow (*lower panel*) of controls (PBS) and bortezomib-treated mice analyzed by flow cytometry. Cells were gated to be CD25⁻. Each diamond or square represents one mouse. Diamonds represent PBS-treated controls; squares denote bortezomib-treated mice. Gray symbols indicate the mice shown in the representative dot plots. Percentages of CD138⁺/cytoplasmic κ/λ -L chain⁺/plasma cells are indicated. *B*, Total numbers and representative wells of ELISPOT results for IgG Abs to DNP-KLH-secreting cells in the spleen (*upper panel*) and the bone marrow (*lower panel*) of controls (PBS) and bortezomib-treated mice. *C*, Total numbers and representative wells of ELISPOT results for IgG Ab-secreting cells in the spleen (*upper panel*) and the bone marrow (*lower panel*) of controls (PBS) and bortezomib-treated mice. *D*, Concentrations of anti-DNP-KLH IgM (*upper panel*) and IgG (*lower panel*) Abs in bortezomib-treated and control (PBS) mice measured by ELISA. *E*, Concentrations of total IgM (*upper panel*) and IgG Abs (*lower panel*) in bortezomib-treated and control (PBS) mice measured by ELISA. Arrows indicate immunizations with DNP-KLH. Data are representative of three independent experiments. Bars in *A*–*C* represent mean values. Error bars depict SD. The Mann–Whitney *U* test was used for all statistical analyses. **p* < 0.05; ***p* < 0.004; ****p* < 0.0004 (*n* = 6 mice/group). Bz, bortezomib.

Statistical analysis

The nonparametric Mann–Whitney *U* test was used for all statistical analyses of results of flow cytometric analyses, ELISPOT, and ELISA. The Student *t* test for heteroschedastic samples was used for statistical analyses of RT-real-time PCR results. All statistical analyses were calculated using SPSS for Windows (SPSS, Munich, Germany).

Results

Reduced plasma cell numbers and Ab concentrations upon bortezomib treatment during immunization with DNP-KLH

To investigate the influence of proteasome inhibition on T-dependent Ab responses, mice were treated with bortezomib for 56 d

beginning simultaneously with the first DNP-KLH immunization. Calculations of total numbers of CD138^{high}/cytoplasmic κ - and λ -L chain⁺/CD25⁻ plasma cells in the spleens and the bone marrows were based on total cell counts and flow cytometric analyses and showed a strong decrease in bortezomib-treated mice when compared with controls (Fig. 1A). Accordingly, ELISPOT assays demonstrated a striking decrease of DNP-KLH-specific IgG- as well as total IgG-secreting cells in the spleens and the bone marrows (Fig. 1B, 1C).

In bortezomib-treated mice there was only a slight increase in anti-DNP-KLH IgM and IgG Ab concentrations upon the first immunization, with no further increase upon the booster immuni-

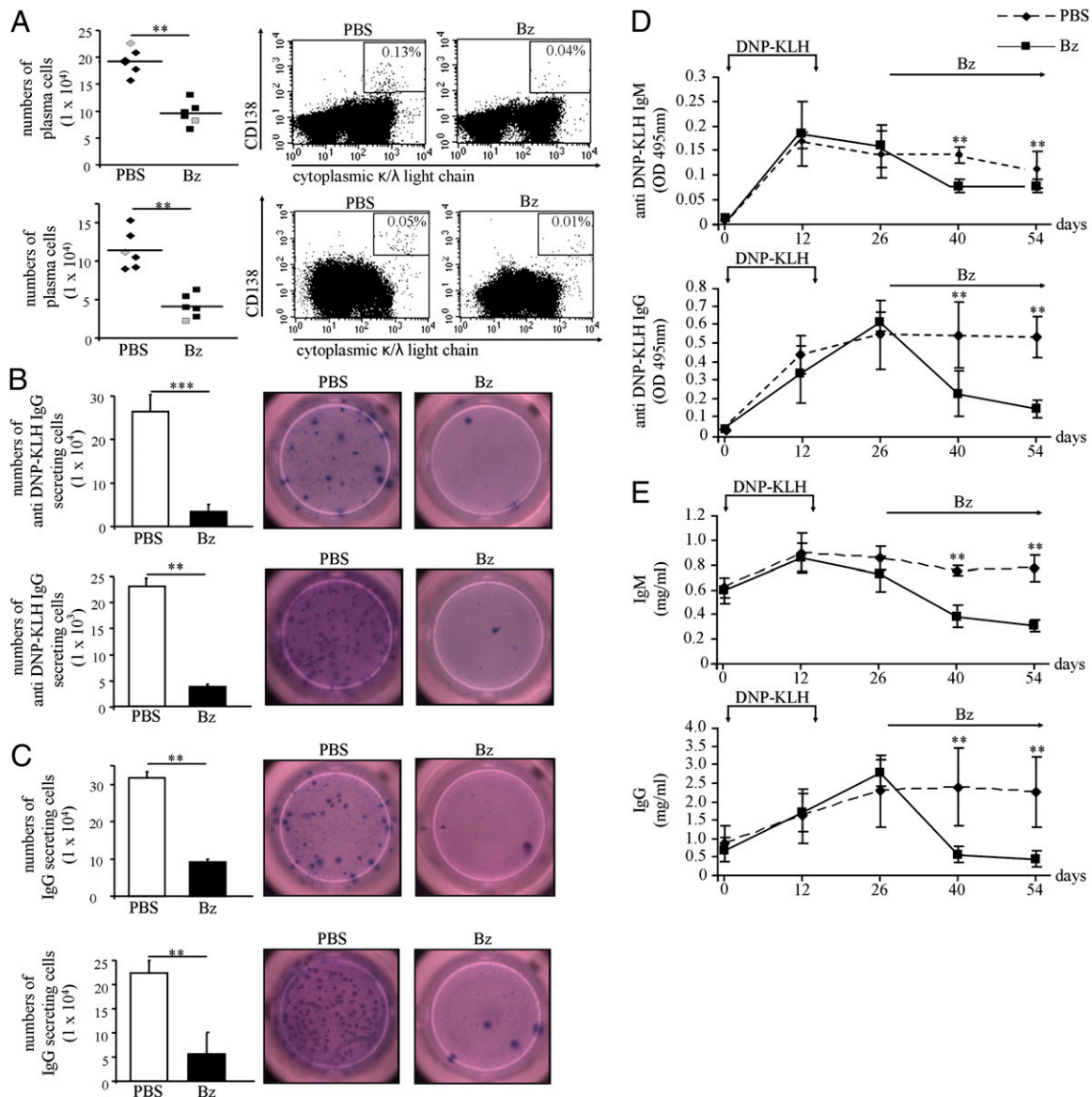


FIGURE 2. Depletion of plasma cells generated by the T-dependent response toward DNP-KLH upon bortezomib treatment. Mice were treated with bortezomib every 72 h from day 28 after the immunization for 28 d. **A**, Total numbers and representative dot plots of CD138^{high}/cytoplasmic κ/λ -L chain⁺/CD25⁻ plasma cells in the spleen (*upper panel*) and the bone marrow (*lower panel*) of control (PBS) and bortezomib-treated mice analyzed by flow cytometry. Cells were gated to be CD25⁻. Each diamond or square represents one mouse. Diamonds represent PBS-treated controls; squares denote bortezomib-treated mice. Gray symbols indicate the mouse that is shown in the representative dot plot. Percentages of CD138^{high}/cytoplasmic κ/λ -L chain⁺ plasma cells are indicated. **B**, Total numbers and representative wells of ELISPOT assays showing cells secreting IgG Abs to DNP-KLH in the spleens (*upper panel*) and the bone marrows (*lower panel*) of controls (PBS) and bortezomib-treated mice. **C**, Total numbers and representative wells of ELISPOT assays for IgG Ab-secreting cells in the spleen (*upper panel*) and the bone marrow (*lower panel*) of controls (PBS) and bortezomib-treated mice. **D**, Levels of anti-DNP-KLH IgM (*upper panel*) and IgG (*lower panel*) Abs in bortezomib-treated and control (PBS) mice measured by ELISA. **E**, Concentrations of total IgM (*upper panel*) and IgG (*lower panel*) Abs in bortezomib-treated and control (PBS) mice measured by ELISA. Arrows indicate immunizations with DNP-KLH. Data are representative of three independent experiments. Error bars represent SD. Bars in A–C represent mean values. Error bars depict SD. The Mann–Whitney *U* test was used for all statistical analyses. **p* < 0.05; ***p* < 0.004; ****p* < 0.0004 (*n* = 6 mice/group). Bz, bortezomib.

zation (Fig. 1D). Serum concentrations of total IgG and IgM displayed only a subtle or transient decrease upon bortezomib treatment, whereas serum concentrations increased in the control group (Fig. 1E). The analyses of IgG subclasses by ELISA revealed differential effects of bortezomib: IgG1, IgG2a, and IgG2b titers were significantly decreased, whereas there was only a trend toward lower IgG3 concentrations (data not shown). Taken together, bortezomib treatment simultaneous with the immunization reduced the T-dependent generation of Abs.

Reduction of pre-existing DNP-KLH-specific plasma cells upon bortezomib treatment

To investigate whether the impaired Ab response toward DNP-KLH acts predominantly in the phase of T-dependent B cell activation and differentiation or is mainly due to the depletion of plasma cells, we started treatment with bortezomib 14 d after the booster immunization when plasma cells had already differentiated. Flow cytometric analyses revealed a significant reduction of CD138^{high}/cytoplasmic κ - and λ -L chain⁺/CD25⁻ plasma cells in the spleens and bone marrows after 28 d of bortezomib application (Fig. 2A). The numbers of cells secreting either anti-DNP-KLH IgG or IgG Abs in both the spleens and the bone marrows were reduced to <20% of vehicle-treated controls as detected by ELISPOT (Fig. 2B, 2C).

The reduction of plasma cell counts upon bortezomib treatment was reflected by markedly lower anti-DNP-KLH IgM and IgG (Fig. 2D) as well as by total IgM and IgG serum concentrations compared with controls (Fig. 2E), having been observed already 14 d after the medication had started. Consistent with the data of the treatment for 56 d, ELISA analyses of IgG subtypes revealed a reduction of IgG1, IgG2a, and IgG2b concentrations, whereas the IgG3 levels remained largely unaffected (data not shown). Hence, also the pre-existing Ab response toward the T-dependent Ag DNP-KLH was decreased by bortezomib application starting 14 d after the last immunization, indicating the depletion of already generated plasma cells.

MZ B cells resist long-term bortezomib treatment

We next determined the sensitivity of different B cell subsets toward bortezomib. Flow cytometric analyses revealed that numbers of B220⁺/CD23^{high}/CD21^{low} follicular B cells were significantly reduced after 56 and 28 d of bortezomib treatment (Fig. 3), but not after 2 d (5). In contrast, B220⁺/CD21^{high}/CD23^{low} MZ B cells were resistant against proteasome inhibition. We even found a trend toward increased absolute numbers of MZ B cells in bortezomib-treated mice (Fig. 3). B220⁺/IgM⁺/IgD⁺ mature B cells, B220⁺/peanut hemagglutinin^{high} germinal center B cells, and B220⁺/IgM⁺/CD5⁺ B1 cells were diminished after 56 and 28 d of bortezomib treatment (data not shown).

Increased IgM Ab titers in MZ B cell-initiated T-independent type 2 responses upon bortezomib treatment

To further investigate our observation that MZ B cells were completely resistant toward proteasome inhibition, we i.v. immunized mice with the T-independent type 2 Ag NIP-Ficoll to preferentially activate MZ B cells and drive their differentiation into plasmablasts. We expected that these highly Ab-secreting cells should become sensitive toward bortezomib. Unexpectedly, bortezomib treatment resulted in a significant increase in anti-NIP-IgM concentrations on day 10 in mice treated with bortezomib from day 0. On day 15 the anti-NIP-IgM decreased to levels of PBS-treated controls. In contrast, titers of mice treated from day 8 were similar to controls (Fig. 4A). Consistent with the increase in anti-NIP-IgM Abs, flow cytometric analyses revealed a trend to-

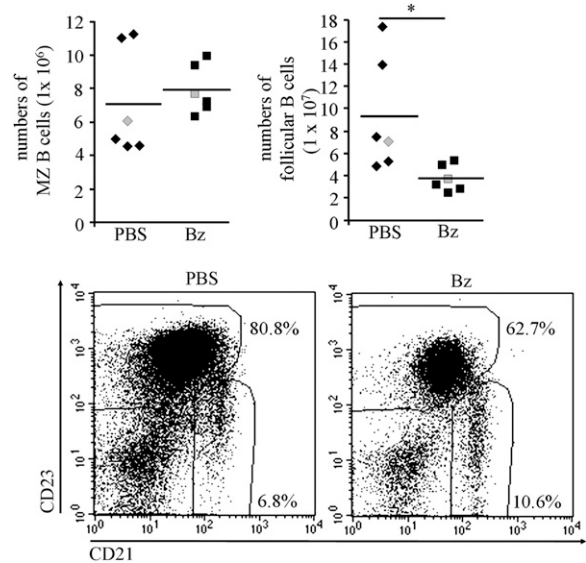


FIGURE 3. Resistance of MZ B cells toward long-term bortezomib administration. Mice were immunized twice with DNP-KLH at intervals of 14 d and treated with bortezomib every 72 h for 56 d. Total numbers and representative dot plots of B220⁺/CD21^{high}/CD23^{low} MZ B cells and of B220⁺/CD23^{high}/CD21^{low} follicular B cells of controls (PBS) and bortezomib-treated mice were analyzed by flow cytometry. Each diamond or square represents one mouse; gray symbols indicate mice that are shown in the representative dot blots. Diamonds represent PBS-treated controls; squares denote bortezomib-treated mice. Frequencies of B220⁺/CD21^{high}/CD23^{low} MZ B cells and of B220⁺/CD23^{high}/CD21^{low} follicular B cells are indicated in percentage of gated B220⁺ B lymphocytes. These data are representative of three independent experiments. Bars represent mean values. The Mann-Whitney *U* test was used for statistical analyses. **p* < 0.05 (*n* = 6 mice/group). Bz, bortezomib.

ward increased numbers of B220⁺/CD21^{high}/CD23^{low} MZ B cells in both long- and short-term bortezomib-treated mice (Fig. 4B). Numbers of CD138^{high}/cytoplasmic IgM^{high}/CD25⁻ plasmablasts that may have predominantly developed from MZ B cells after NIP-Ficoll stimulation were not reduced after 5 d of treatment (Fig. 4C). However, anti-NIP-IgG concentrations, which were predominantly of the IgG3 isotype, remained constantly below controls in both bortezomib-treated groups (Fig. 4D). These data indicate that the MZ B cell initiated T-independent type 2 IgM response is completely resistant toward proteasome inhibition during the initial phase.

Induction of immunoproteasomal subunits in MZ B cells upon bortezomib treatment

To investigate whether the resistance of MZ B cells toward bortezomib is due to abundant expression of proteasomes, we determined the chymotrypsin-like activity of the 26S proteasome. MZ and follicular B cells displayed a similar proteasomal activity, which was markedly lower than proteasomal activities in splenic and bone marrow plasma cells. Plasmablasts exhibited a much higher proteasomal activity than did all other B cell subsets, including plasma cells (Fig. 5A). This extremely high proteasomal activity in plasmablasts is consistent with the induction of proteasomal capacity in LPS-induced plasmablasts previously described by Cascio et al. (14) and might represent a general feature of plasmablasts.

The standard 26S proteasome is composed of three different proteolytically active subunits, β 1, β 2, and β 5. In the immunoproteasomes these subunits are replaced by their corresponding

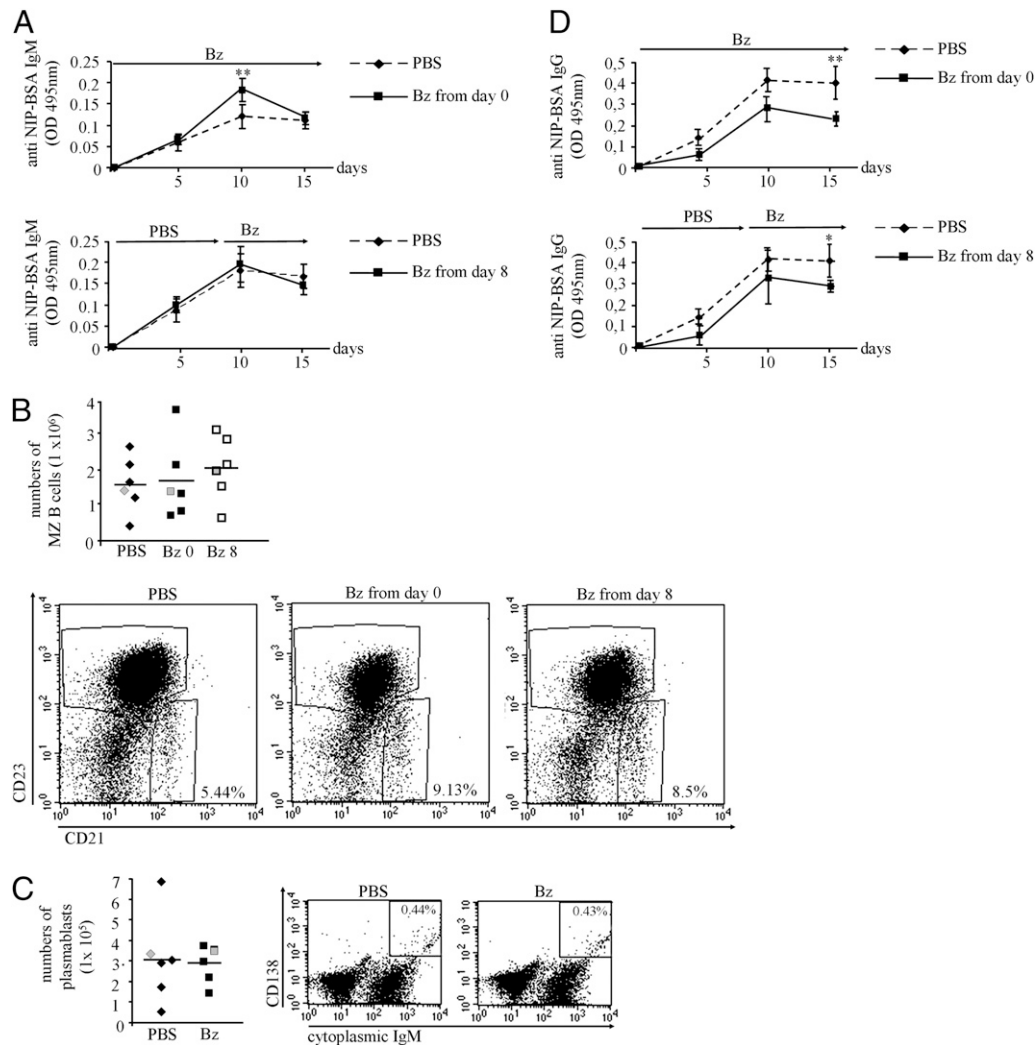


FIGURE 4. MZ B cells and the early phase of the T-independent type 2 response resist bortezomib. Mice were immunized with NIP-Ficoll and treated for 5 and 16 d, respectively. *A*, Concentrations of anti-NIP IgM Abs of bortezomib-treated and control (PBS) mice measured by ELISA. Mice were treated with bortezomib either starting simultaneously with the immunization (day 0; *upper panel*) or from day 8 after the immunization (*lower panel*). *B*, Total numbers and representative dot plots of B220⁺/CD21^{high}/CD23^{low} MZ B cells of controls (PBS) from day 0 (*middle*) and from day 8 bortezomib-treated mice (*right*) analyzed by flow cytometry. Each diamond or square represents one mouse. Diamonds represent PBS-treated controls; closed squares denote mice treated with bortezomib from day 0; open quadrates depict mice treated with bortezomib from day 8. Gray symbols indicate mice shown in the dot plots. Percentages of B220⁺/CD21^{high}/CD23^{low} MZ B cells are indicated. *C*, Total numbers and representative dot plots of CD138⁺/cytoplasmic IgM⁺/CD25⁻ plasmablasts in the spleens of control (PBS) and bortezomib-treated mice after 5 d of bortezomib treatment analyzed by flow cytometry. Beginning simultaneously with the immunization mice were treated with bortezomib every 48 h for 5 d. Each diamond or square represents one mouse. Diamonds represent PBS-treated controls; squares denote bortezomib-treated mice. Gray symbols indicate mice shown in the dot plots. Percentages of splenic CD138⁺/cytoplasmic IgM⁺/CD25⁻ plasmablasts are indicated. *D*, Concentrations of anti-NIP IgG Abs of bortezomib-treated and control (PBS) mice measured by ELISA. Mice were treated with bortezomib simultaneously with the immunization (day 0; *upper panel*) or from day 8 after the immunization (*lower panel*). Bz 0, bortezomib from day 0; Bz 8, bortezomib from day 8. Data are representative of three independent experiments. Error bars represent SD. Bars in *B* represent mean values. The Mann-Whitney *U* test was used for all statistical analyses. **p* < 0.05; ***p* < 0.004 (*n* = 6 mice/group).

subunits LMP2, LMP7, and MECL-1 (15). Bortezomib predominantly inhibits the chymotrypsin-like activity of the $\beta 5$ subunit, but also the proteolytic activity of the immunoproteasome (16). There is evidence that malignant B cell lines, which are insensitive toward bortezomib, display increased expression of the $\beta 5$ and LMP2 subunits (17). Thus, we investigated mRNA and protein levels of the PSMB5-encoded $\beta 5$ subunit of LMP2 and of LMP7 by relative RT-real-time PCR and immunoblotting, respectively. MZ B cells showed significantly lower amounts of PSMB5 mRNA than did follicular B and plasma cells (Fig. 5*B*). After 4 h of bortezomib treatment there was no significant increase of transcripts to PSMB5 in MZ B cells, whereas transcripts to PSMB5 were strongly induced in plasma cells (Fig. 5*B*). The $\beta 5$ protein

was low in MZ and follicular B cells (data not shown). MZ B cells showed low levels of transcripts to LMP2 and LMP7. Intriguingly, the mRNA concentrations of LMP2 and LMP7 were increased in MZ B cells upon bortezomib exposure. In contrast, LMP2 and LMP7 mRNA strongly decreased in follicular B and plasma cells upon bortezomib treatment. Consistent with the mRNA level, LMP2 protein concentration strongly decreased in follicular B cells upon bortezomib treatment, whereas LMP7 protein concentration remained unchanged (Fig. 5*B*, 5*C*). LMP2 and LMP7 protein concentrations remained stable in MZ B cells. These data indicate that MZ B cells constitutively express very low amounts of immunoproteasome subunits, which are rapidly induced by bortezomib and may counteract bortezomib-induced ER stress.

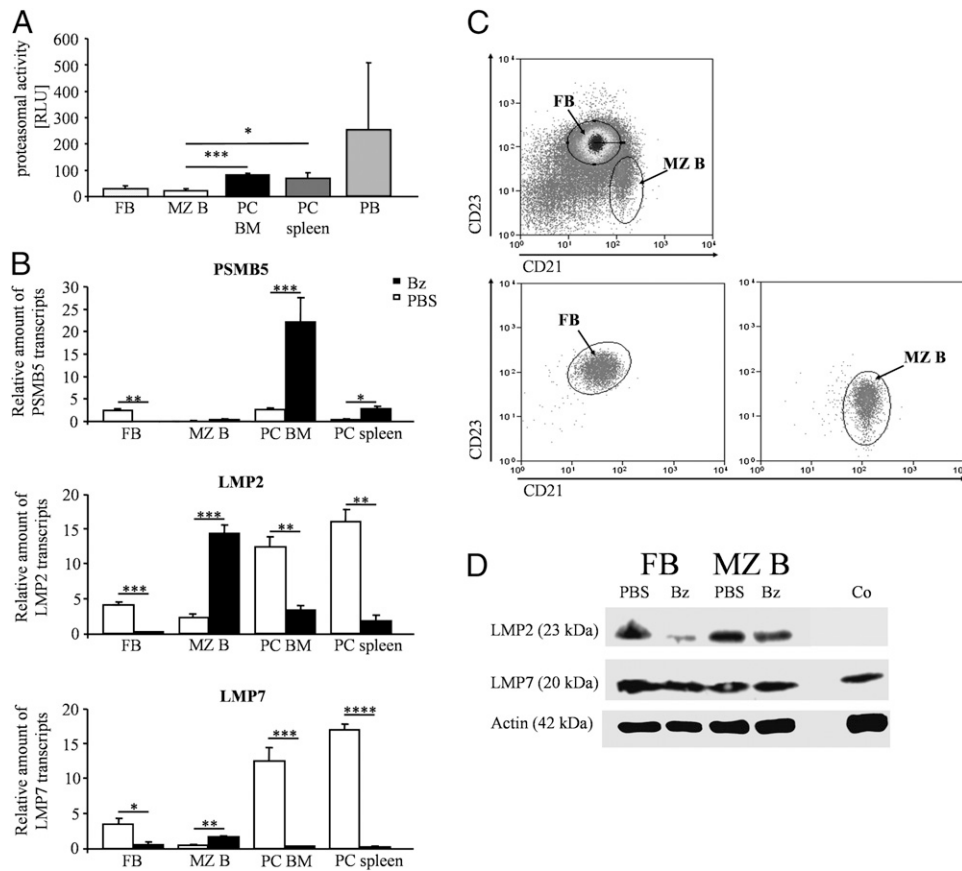


FIGURE 5. Proteasomal activity and expression of regular and immunoproteasomal subunits in MZ B cells, follicular B cells, and plasma cells. *A*, Luminescence-based measurement (RLU with background subtracted) of the chymotrypsin-like proteasomal activity in follicular B, MZ B, splenic, and bone marrow plasma cells as well as plasmablasts. *B*, Relative RT-real-time PCR quantification of mRNA levels of the proteasomal $\beta 5$ subunit encoded by PSMB5 as well as the immunoproteasomal subunits LMP2 and LMP7 in follicular B, MZ B, splenic, and bone marrow plasma cells. The white bar graphs show levels of controls (PBS); the black bar graphs represent transcriptional changes 4 h after a single bortezomib injection compared with a standard comprised of pooled RNA from total splenocytes. *C*, Representative cell sorting data and reanalyses of MZ and follicular B cells. Cells were gated to be B220⁺. CD21^{high}/CD23^{low} MZ B and CD23^{high}/CD21^{low} follicular B cells were sorted with purity >98%. *D*, Immunoblot analysis of total cell lysates of MZ and follicular B cells. Changes in expression of LMP2 and LMP7 8 h after a single bortezomib treatment. Tunicamycin-treated HeLa cells served as control. Data are representative of three independent experiments. Error bars represent SD. The Student *t* test for heteroschedastic samples was used for all statistical analyses. **p* < 0.05; ***p* < 0.004; ****p* < 0.0002; *****p* < 0.00004. Bz, bortezomib; FB, follicular B cells; MZ B, MZ B cells; PC BM, plasma cells from the bone marrow; PC spleen, plasma cells from the spleen.

Absence of terminal UPR activation in MZ B cells after bortezomib treatment

Proteasome inhibition leads to inhibition of NF- κ B activation due to blockade of I κ B degradation. To investigate whether NF- κ B activity may be involved in the resistance of MZ B cells against bortezomib, we measured the relative amounts of I κ B α transcripts, which are strongly induced by NF- κ B. The levels of I κ B α mRNA were lower in MZ B cells than in follicular B and in plasma cells, indicating lower NF- κ B activity in MZ B cells compared with follicular B cells and plasma cells. However, 4 h after bortezomib treatment, I κ B α mRNA concentrations increased in MZ B cells but decreased in follicular B as well as in plasma cells (Fig. 6A). Hence, unexpectedly, and in contrast to other B cell subsets, MZ B cells can activate the anti-apoptotic transcription factor NF- κ B in response to proteasome inhibition.

To assess the ER stress response in MZ B cells and in follicular B and plasma cells, we compared the mRNA and protein concentrations of UPR-related survival and proapoptotic factors by relative RT-real-time PCR and immunoblotting, respectively. The ER-resident molecular chaperone BiP binds to unfolded proteins and indicates activation of the anti-apoptotic UPR (18). When comparing BiP mRNA concentrations, we observed that BiP was

abundant in plasma cells, whereas MZ B and follicular B cells showed low BiP mRNA levels. Four hours after bortezomib application BiP mRNA increased in MZ B cells, but strongly decreased in plasma cells and slightly in follicular B cells. Accordingly, BiP protein increased in MZ B cells after bortezomib injection, but it decreased in follicular B cells (Fig. 6). The transcription factor CHOP was shown to exert proapoptotic activity in certain systems (19); however, in B lymphocytes there is no evidence of CHOP directly contributing to apoptosis (20). Nevertheless, CHOP activation can serve as an indicator for activation of the terminal UPR and consequent apoptosis. CHOP mRNA was very low in plasma cells and virtually absent in follicular and MZ B cells. Within 4 h after bortezomib treatment the amount of transcripts to CHOP rose >180-fold in bone marrow and >50-fold in splenic plasma cells. In contrast, CHOP mRNA and protein remained undetectable in MZ B cells upon bortezomib treatment (Fig. 6). Despite an increase of CHOP mRNA, protein concentrations remained undetectable in follicular B cells (Fig. 6), which are not or just slightly decreased upon a single bortezomib injection and only moderately decreased after long-term treatment.

Members of the Bcl-2 family, such as the proapoptotic Bax protein, contribute to bortezomib-mediated apoptosis induction

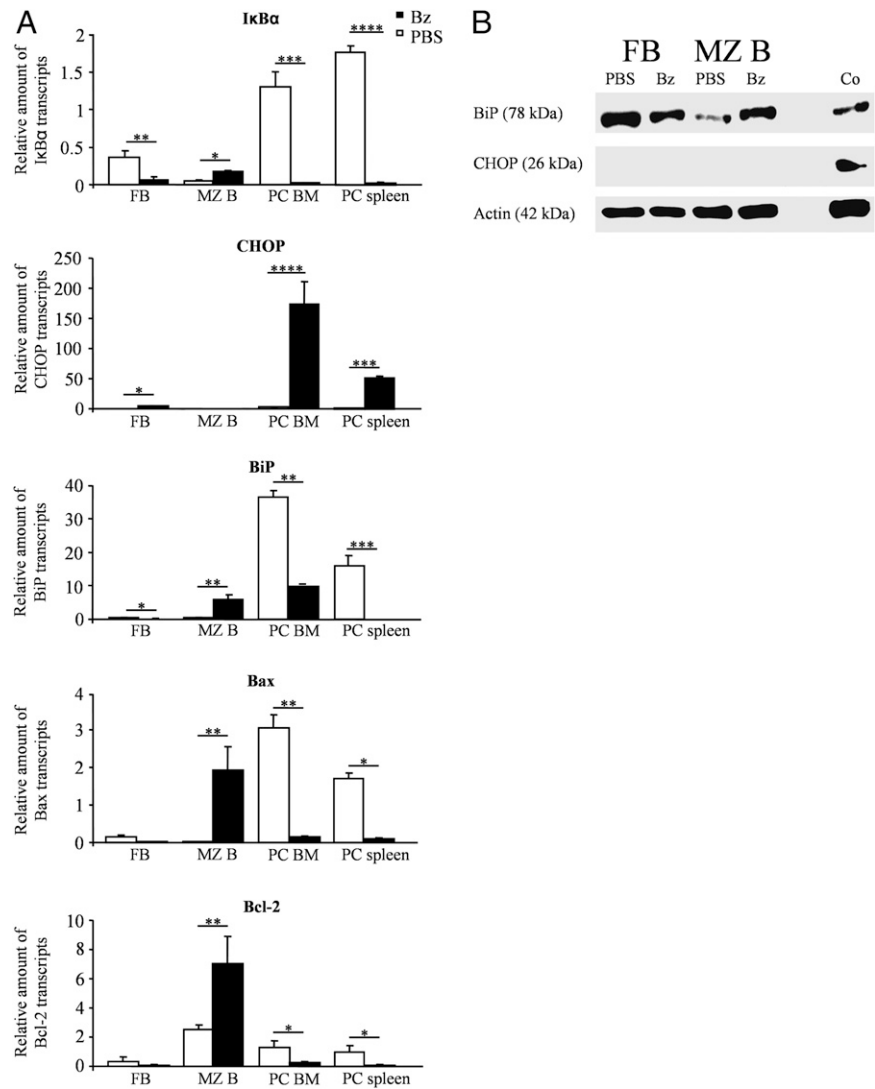


FIGURE 6. Absence of proapoptotic UPR activation in MZ B cells after bortezomib administration. **A**, Relative RT-real-time PCR quantification of mRNA levels of UPR-related pro- and antiapoptotic factors in follicular B, MZ B, spleen, and bone marrow plasma cells. The white bar graphs show levels of controls (PBS); the black bar graphs represent transcriptional changes 4 h after a single bortezomib injection compared with a standard comprised of pooled RNA from total splenocytes. Relative amounts of transcripts for IκBα, CHOP, BiP, Bax, and Bcl-2. **B**, Immunoblot analysis of total cell lysates of MZ and FB cells. Changes in expression of CHOP and BiP 8 h after a single bortezomib injection. Tunicamycin-treated HeLa cells served as control. Data are representative of three independent experiments. Error bars represent SD. The Student *t* test for heteroschedastic samples was used for all statistical analyses. **p* < 0.04; ***p* < 0.004; ****p* < 0.0003; *****p* < 0.00004 (*n* = 3 mice/group). Bz, bortezomib; FB, follicular B cells; MZ B, MZ B cells; PC BM, plasma cells from the bone marrow; PC spleen, plasma cells from the spleen.

(21). The basal amount of Bax transcripts was relatively high in plasma cells. In contrast, mRNA of the antiapoptotic factor Bcl-2 was expressed at highest concentrations in MZ B cells and somewhat less in plasma cells. Four hours after bortezomib administration mRNA expression levels of both Bax and Bcl-2 were increased in MZ B cells, whereas they were decreased in other B cell subsets (Fig. 6A). Despite mRNA induction, Bax protein remained absent in MZ B cells after bortezomib treatment (data not shown). In summary, only in MZ B cells, but not in other B cell subsets, did bortezomib induce NF-κB activation and other survival factors without activation of the terminal UPR.

MZ B cells maintain bortezomib resistance when released into the blood

Gong et al. (22) showed that resistance of MZ B cells toward treatment with anti-CD20 Abs is due to their cellular microenvironment. To analyze the contribution of the microenvironment to the bortezomib resistance, we mobilized MZ B cells into the peripheral blood by injection of Abs to the integrin α₄-chain and the integrin α_L-chain after immunization with NIP-Ficoll. Bortezomib or PBS was simultaneously administered. We performed flow cytometric analyses of venous blood 2, 6, and 24 h after treatment. After 2 h IgM⁺/B220⁺/CD21^{high}/CD23^{low} MZ B cells were detectable in the peripheral blood, representing ~3.5% of total blood lymphocytes. As expected, follicular B cells were also mobilized

and their counts in the peripheral blood increased (Fig. 7). Importantly, MZ B cells that were mobilized into the circulation did not decline 4 and 6 h after bortezomib injection when compared with mice treated with PBS, indicating persistent resistance toward bortezomib (Fig. 7). Of note, already 2 h after the treatment, numbers of B220^{low}/CD138^{high}/cytoplasmic κ- and λ-L chain⁺ plasma cells in the blood were diminished by 50%. Additionally, there was a trend toward decreased numbers of follicular B cells upon bortezomib treatment (data not shown). In summary, displacing MZ B cells from the spleen into the peripheral blood did not overcome bortezomib resistance. However, this does not exclude contribution of long-lasting protective effects of the microenvironment.

Discussion

We compared the consequence of bortezomib administration on plasma cells and Ab titers in T-dependent and T-independent type 2 responses. Proteasome inhibition markedly reduced the numbers of plasma cells as well as Ab titers in T-dependent responses. Elimination of plasma cells occurred within 8 h after bortezomib injection (V.R. Lang, S. Meister, R.E. Voll, unpublished data). The depletion of pre-existing plasma cells indicates that bortezomib may suppress T-dependent responses mainly by targeting plasma cells. Nevertheless, there may be an additional suppressive effect of bortezomib on T and dendritic cells impairing plasma cell

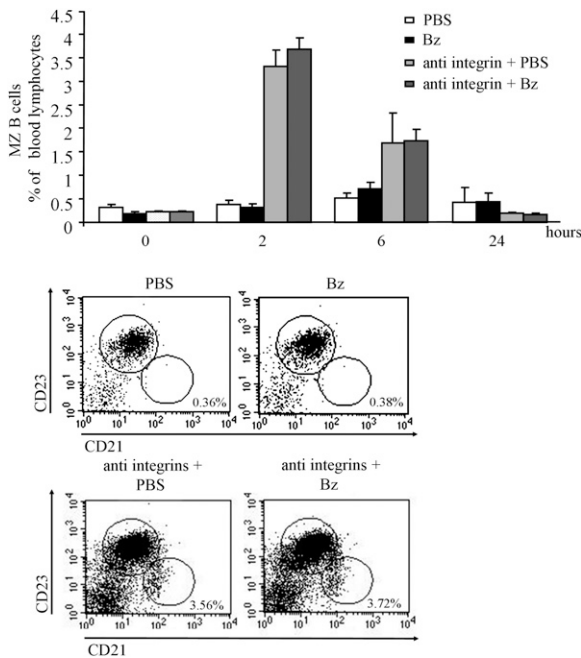


FIGURE 7. Mobilization of MZ B cells to the peripheral blood does not render them sensitive toward bortezomib. NIP-Ficoll-immunized mice were treated with anti-integrin Abs to mobilize MZ B cells into the peripheral blood. Simultaneously, bortezomib was administered. Controls received either PBS or bortezomib without integrin blockade. Bar diagram shows mean frequencies in percentage and representative dot plots (2 h after treatment) of IgM⁺/B220⁺/CD21^{high}/CD23^{low} MZ B cells of PBS- versus bortezomib-treated mice with (*upper panel*) or without anti-integrin Ab treatment (*lower panel*) in venous blood analyzed by flow cytometry. These data are representative of two independent experiments ($n = 3$ mice/group).

differentiation (23), although the numbers of T helper and dendritic cells were not significantly decreased within the first 14 d of treatment (data not shown and Ref. 5). Moreover, we previously demonstrated that bortezomib inhibited Ag-induced mouse T cell proliferation only slightly (13), whereas others reported more pronounced effects of bortezomib on the function of human CD4⁺ T cells (24).

Bortezomib application clearly dampened T-dependent immune responses by targeting short- and long-lived plasma cells, but it did not obviate the generation of IgM Ab-secreting cells in response to NIP-Ficoll.

The Ab response to i.v. injected NIP-Ficoll is predominantly mediated by MZ B cells that differentiate into plasmablasts, which produce large amounts of Ag-specific IgM (10). Unexpectedly, bortezomib treatment did not affect the MZ B cell response to NIP-Ficoll. Cascio et al. (14) described an impaired formation of IgM Abs to i.p. applied NIP-Ficoll upon bortezomib treatment, with Ab titers being significantly decreased beyond day 15. When we immunized mice i.p. as performed by Cascio et al. we also observed significantly reduced anti-NIP IgM and IgG levels (V.R. Lang, S. Meister, R.E. Voll, data not shown). It was previously demonstrated that i.p. administered NIP-Ficoll predominantly stimulates peritoneal B1 cells, whereas i.v. injected NIP-Ficoll preferentially activates splenic MZ B cells (11). Upon i.p. injection of bortezomib, peritoneal B220⁺/CD5⁺/CD43⁺ B1a cells as well as B220⁺/CD5⁻/CD43⁻ B1b cells were reduced to <20% of controls after 16 d (V.R. Lang et al., manuscript in preparation). This high sensitivity of peritoneal B1 cells toward bortezomib may account for the impaired development of Abs to i.p. applied NIP-Ficoll. Furthermore, compared with the experiments performed by Cascio et al. (14)

we applied bortezomib i.v. at the 1.5-fold dosage. The elevated anti-NIP-specific IgM concentrations despite the higher bortezomib dosage emphasize the resistance of MZ B cell-originated T-independent type 2 responses. However, it remains unclear why bortezomib leads to even increased IgM responses to NIP-Ficoll. In contrast, NIP-specific IgG levels of bortezomib-treated mice constantly remained below controls. After 14 d of treatment, splenic plasma cells were predominantly depleted (data not shown). MZ B cells differentiate mainly into short-lived plasma cells (25), and it is not yet clear whether they also give rise to long-lived plasma cells. NIP-specific IgG may either arise from some class switching of activated MZ B cell-derived plasma cells or from bortezomib-sensitive activated B1 cells, which contribute to the persisting IgG response to NIP-Ficoll (26). Therefore, reduced numbers of B1 cells upon bortezomib treatment may account for the reduced NIP-specific IgG levels, which were mainly of the IgG3 isotype, consistent with previous results (26).

One reason for the resistance of the early T-independent type 2 response toward bortezomib might be that in contrast to plasma cells, proapoptotic UPR pathways were not activated in MZ B cells by proteasome inhibition. As we reported recently, cells producing large amounts of Ig are especially sensitive toward bortezomib, because proteasome blockade induces ER stress and thereby activates proapoptotic UPR pathways (6). More recently, Bianchi et al. (27) pointed out that the ratio of load versus capacity determines the actual sensitivity of myeloma cell lines toward proteasome inhibitors. We observed that plasma cells generated by the response to DNP-KLH were affected by mechanisms similar to those eliminating their autoreactive counterparts (5). The drastic increase in mRNA levels of the terminal UPR-related factor CHOP, as well as the decrease of antiapoptotic BiP and Bcl-2 after bortezomib administration, indicated that plasma cells were depleted by the activation of the terminal UPR. Resting MZ B cells were the only B cell population that was not at all altered after 56 d of bortezomib treatment, whereas follicular B cells, which were largely resistant to one or two injections of bortezomib, were decreased by ~50% after treatment lasting 28 or 56 d. We expected that MZ B cells should become sensitive to ER stress caused by proteasome blockade upon induction of Ab synthesis, despite their highly developed ER with an excess of chaperones, which enables them to rapidly produce high amounts of Abs upon pathogen encounter (28). This feature may help to rescue them from excessive ER stress. In line with this speculation, bortezomib did not induce CHOP in MZ B cells. Instead, antiapoptotic factors such as BiP and Bcl-2 were upregulated and may contribute to the resistance of MZ B cells toward bortezomib. Furthermore, the activity of the antiapoptotic transcription factor NF- κ B was increased in MZ B cells upon bortezomib exposure. However, the mechanism of bortezomib-induced NF- κ B activation in MZ B cells remains elusive. While the UPR usually activates NF- κ B, bortezomib should inhibit NF- κ B activation, at least via the classical pathway. Increased NF- κ B activation may explain enhanced Bcl-2 expression in MZ B cells upon bortezomib exposure.

In addition to upregulation of NF- κ B, we observed an increase in mRNA concentrations of immunoproteasomal subunits in MZ B cells upon bortezomib administration. However, concentrations of LMP2 and LMP7 proteins remained unchanged 8 h after bortezomib treatment. This might be due to altered translation upon proteasome blockade or due to the relatively long half-life of proteasomal subunits. Nevertheless, LMP2 protein concentrations strongly declined in the partially bortezomib-sensitive follicular B cells. Thus, MZ B cells may be able to counteract bortezomib by enhancing the capacity of protein degradation and, thereby, to prevent overwhelming ER stress, as it has been shown by Bianchi

et al. (27). However, the induction of immunoproteasomal subunits alone might not fully explain why MZ B cells resist proteasome blockade. Plasma cells showed higher basal chymotrypsin-like proteasomal activity than did MZ B cells, and the mRNA concentrations of the $\beta 5$ subunit were stongly increased after bortezomib treatment. As shown previously, increased concentrations of the $\beta 5$ subunit can protect cells from bortezomib-induced cell death (29). However, in the case of plasma cells, this compensatory mechanism may not be sufficient to prevent the terminal UPR.

Furthermore, we asked whether MZ B cells received survival signals from the specialized MZ microenvironment, which may contribute to their bortezomib resistance. In contrast to the depletion of MZ B cells by anti-CD20 Abs after mobilization out of the spleen (22), mobilized MZ B cells remained resistant to bortezomib at least during the first 6 h. After 24 h MZ B cells had disappeared from the blood again, but we could not distinguish whether this was due to depletion or to resettlement. Hence, it remains elusive as to which stimuli or cellular properties in particular activate potential resistance mechanisms such as induction of immunoproteasome subunits and antiapoptotic UPR pathways in MZ B cells. As noncanonical NF- κ B signaling is crucial for MZ B cell development (30), it is possible that activation of this pathway might contribute to the resistance toward bortezomib (31). In this respect it is noteworthy that we have preliminary evidence that noncanonical NF- κ B signaling is not inhibited by therapeutic concentrations of bortezomib (D. Mielenz, V.R. Lang, S. Meister, R.E. Voll, unpublished data).

Our findings about the differential sensitivity of the T-dependent and T-independent type 2 responses have an important impact for the clinical use of bortezomib. The suppression of T-dependent Ab responses points toward applications in autoantibody-mediated diseases (32) as well as in transplantation medicine to suppress Ab-mediated rejection (33). In fact, Everly et al. (34) reported that bortezomib reduced donor-specific anti-HLA-Ab levels in human kidney transplanted patients refractory toward conventional treatments. Another useful aspect of proteasome inhibition as a therapeutic approach in transplantation medicine might be that bortezomib ameliorates graft-versus-host disease in murine transplantation models when combined with TNF- α blockade or depletion of CD4⁺ T cells (35). The fact that bortezomib treatment leaves T-independent type 2 immune responses intact, which protect the organism against blood-borne pathogens such as encapsulated bacteria, may represent an important advantage for its administration as a rather selective immunosuppressant. Commonly applied cytostatic drugs such as cyclophosphamide cause a severe reduction and slow recovery of granulocytes, lymphocytes, and MZ B cells in rats (36). In contrast, bortezomib appears to leave at least the marginal zone B cell-mediated immediate antibacterial defense intact.

Acknowledgments

We thank B. Frey and D. Graef for assistance as well as U. Appelt for expert cell sorting.

Disclosures

S.M. and R.E.V. have a patent application for the use of proteasome inhibitors. The other authors have no financial conflicts of interests.

References

- Schwartz, R. N., and M. Vozniak. 2008. Current and emerging treatments for multiple myeloma. *J. Manag. Care Pharm.* 14(7, Suppl):12–19.
- Ludwig, H., D. Khayat, G. Giaccone, and T. Facon. 2005. Proteasome inhibition and its clinical prospects in the treatment of hematologic and solid malignancies. *Cancer* 104: 1794–1807.
- Adams, J. 2004. The proteasome: a suitable antineoplastic target. *Nat. Rev. Cancer* 4: 349–360.
- Sunwoo, J. B., Z. Chen, G. Dong, N. Yeh, C. Crowl Bancroft, E. Sausville, J. Adams, P. Elliott, and C. Van Waes. 2001. Novel proteasome inhibitor PS-341 inhibits activation of nuclear factor- κ B, cell survival, tumor growth, and angiogenesis in squamous cell carcinoma. *Clin. Cancer Res.* 7: 1419–1428.
- Neubert, K., S. Meister, K. Moser, F. Weisel, D. Maseda, K. Amann, C. Wieth, T. H. Winkler, J. R. Kalden, R. A. Manz, and R. E. Voll. 2008. The proteasome inhibitor bortezomib depletes plasma cells and protects mice with lupus-like disease from nephritis. *Nat. Med.* 14: 748–755.
- Meister, S., U. Schubert, K. Neubert, K. Herrmann, R. Burger, M. Gramatzki, S. Hahn, S. Schreiber, S. Wilhelm, M. Herrmann, et al. 2007. Extensive immunoglobulin production sensitizes myeloma cells for proteasome inhibition. *Cancer Res.* 67: 1783–1792.
- Obeng, E. A., L. M. Carlson, D. M. Gutman, W. J. Harrington, Jr., K. P. Lee, and L. H. Boise. 2006. Proteasome inhibitors induce a terminal unfolded protein response in multiple myeloma cells. *Blood* 107: 4907–4916.
- Fribley, A., and C. Y. Wang. 2006. Proteasome inhibitor induces apoptosis through induction of endoplasmic reticulum stress. *Cancer Biol. Ther.* 5: 745–748.
- Mateos, M. V., and J. F. San Miguel. 2007. Bortezomib in multiple myeloma. *Best Pract. Res. Clin. Haematol.* 20: 701–715.
- Pillai, S., A. Cariappa, and S. T. Moran. 2005. Marginal zone B cells. *Annu. Rev. Immunol.* 23: 161–196.
- Martin, F., A. M. Oliver, and J. F. Kearney. 2001. Marginal zone and B1 B cells unite in the early response against T-independent blood-borne particulate antigens. *Immunity* 14: 617–629.
- Zandvoort, A., and W. Timens. 2002. The dual function of the splenic marginal zone: essential for initiation of anti-TI-2 responses but also vital in the general first-line defense against blood-borne antigens. *Clin. Exp. Immunol.* 130: 4–11.
- Maseda, D., S. Meister, K. Neubert, M. Herrmann, and R. E. Voll. 2008. Proteasome inhibition drastically but reversibly impairs murine lymphocyte development. *Cell Death Differ.* 15: 600–612.
- Cascio, P., L. Oliva, F. Cerruti, E. Mariani, E. Pasqualetto, S. Cenci, and R. Sitia. 2008. Dampening Ab responses using proteasome inhibitors following in vivo B cell activation. *Eur. J. Immunol.* 38: 658–667.
- Kloetzel, P. M. 2004. The proteasome and MHC class I antigen processing. *Biochim. Biophys. Acta* 1695: 225–233.
- Altun, M., P. J. Galardy, R. Shringarpure, T. Hideshima, R. LeBlanc, K. C. Anderson, H. L. Ploegh, and B. M. Kessler. 2005. Effects of PS-341 on the activity and composition of proteasomes in multiple myeloma cells. *Cancer Res.* 65: 7896–7901.
- Busse, A., M. Kraus, I. K. Na, A. Rietz, C. Scheibenbogen, C. Driessen, I. W. Blau, E. Thiel, and U. Keilholz. 2008. Sensitivity of tumor cells to proteasome inhibitors is associated with expression levels and composition of proteasome subunits. *Cancer* 112: 659–670.
- Gething, M. J. 1999. Role and regulation of the ER chaperone BiP. *Semin. Cell Dev. Biol.* 10: 465–472.
- Zinszner, H., M. Kuroda, X. Wang, N. Batchvarova, R. T. Lightfoot, H. Remotti, J. L. Stevens, and D. Ron. 1998. CHOP is implicated in programmed cell death in response to impaired function of the endoplasmic reticulum. *Genes Dev.* 12: 982–995.
- Masciarelli, S., A. M. Fra, N. Pengo, M. Bertolotti, S. Cenci, C. Fagioli, D. Ron, L. M. Hendershot, and R. Sitia. 2010. CHOP-independent apoptosis and pathway-selective induction of the UPR in developing plasma cells. *Mol. Immunol.* 47: 1356–1365.
- Fennell, D. A., A. Chacko, and L. Mutti. 2008. BCL-2 family regulation by the 20S proteasome inhibitor bortezomib. *Oncogene* 27: 1189–1197.
- Gong, Q., Q. Ou, S. Ye, W. P. Lee, J. Cornelius, L. Diehl, W. Y. Lin, Z. Hu, Y. Lu, Y. Chen, et al. 2005. Importance of cellular microenvironment and circulatory dynamics in B cell immunotherapy. *J. Immunol.* 174: 817–826.
- Zinser, E., S. Rössner, L. Littmann, D. Lüftenegger, U. Schubert, and A. Steinkasserer. 2009. Inhibition of the proteasome influences murine and human dendritic cell development in vitro and in vivo. *Immunobiology* 214: 843–851.
- Berges, C., H. Haberstock, D. Fuchs, M. Miltz, M. Sadeghi, G. Opelz, V. Daniel, and C. Naujokat. 2008. Proteasome inhibition suppresses essential immune functions of human CD4⁺ T cells. *Immunology* 124: 234–246.
- Lopes-Carvalho, T., and J. F. Kearney. 2004. Development and selection of marginal zone B cells. *Immunol. Rev.* 197: 192–205.
- Hsu, M. C., K. M. Toellner, C. G. Vinuesa, and I. C. MacLennan. 2006. B cell clones that sustain long-term plasmablast growth in T-independent extra-follicular antibody responses. *Proc. Natl. Acad. Sci. USA* 103: 5905–5910.
- Bianchi, G., L. Oliva, P. Cascio, N. Pengo, F. Fontana, F. Cerruti, A. Orsi, E. Pasqualetto, A. Mezghrani, V. Calbi, et al. 2009. The proteasome load versus capacity balance determines apoptotic sensitivity of multiple myeloma cells to proteasome inhibition. *Blood* 113: 3040–3049.
- Gunn, K. E., and J. W. Brewer. 2006. Evidence that marginal zone B cells possess an enhanced secretory apparatus and exhibit superior secretory activity. *J. Immunol.* 177: 3791–3798.
- Ruckrich, T., M. Kraus, J. Gogel, A. Beck, H. Ovaa, M. Verdoes, H. S. Overkleeft, H. Kalbacher, and C. Driessen. 2009. Characterization of the ubiquitin-proteasome system in bortezomib-adapted cells. *Leukemia* 23: 1098–1105.
- Weih, D. S., Z. B. Yilmaz, and F. Weih. 2001. Essential role of RelB in germinal center and marginal zone formation and proper expression of homing chemokines. *J. Immunol.* 167: 1909–1919.
- Allen, C., K. Saigal, L. Nottingham, P. Arun, Z. Chen, and C. Van Waes. 2008. Bortezomib-induced apoptosis with limited clinical response is accompanied by

- inhibition of canonical but not alternative nuclear factor- κ B subunits in head and neck cancer. *Clin. Cancer Res.* 14: 4175–4185.
32. Voll, R., and F. Hiepe. 2009. Depletion of plasma cells: a novel strategy in the therapy of systemic lupus erythematosus in mice and man. *Z. Rheumatol.* 68: 150–153.
 33. Sun, K., M. Li, T. J. Sayers, L. A. Welniak, and W. J. Murphy. 2008. Differential effects of donor T-cell cytokines on outcome with continuous bortezomib administration after allogeneic bone marrow transplantation. *Blood* 112: 1522–1529.
 34. Everly, M. J., J. J. Everly, B. Susskind, P. Brailey, L. J. Arend, R. R. Alloway, P. Roy-Chaudhury, A. Govil, G. Mogilishetty, A. H. Rike, et al. 2009. Proteasome inhibition reduces donor-specific antibody levels. *Transplant. Proc.* 41: 105–107.
 35. Sun, K., D. E. Wilkins, M. R. Anver, T. J. Sayers, A. Panoskaltis-Mortari, B. R. Blazar, L. A. Welniak, and W. J. Murphy. 2005. Differential effects of proteasome inhibition by bortezomib on murine acute graft-versus-host disease (GVHD): delayed administration of bortezomib results in increased GVHD-dependent gastrointestinal toxicity. *Blood* 106: 3293–3299.
 36. Zandvoort, A., M. E. Lodewijk, P. A. Klok, P. M. Dammers, F. G. Kroese, and W. Timens. 2001. Slow recovery of follicular B cells and marginal zone B cells after chemotherapy: implications for humoral immunity. *Clin. Exp. Immunol.* 124: 172–179.